

The CD spectra of **1** (hydratropic acid), **3** (mandelic acid), **5** (atrolactic acid), and the corresponding esters have been reported by Barth *et al.*,<sup>1</sup> and Korver<sup>4,5</sup> has reported the CD spectra of a wide variety of mandelic acid derivatives. Although tentative band (CD) assignments and spectra-structure relationships have been offered for these systems studied in solution, there remains considerable uncertainty regarding the interpretation of their CD spectra.

#### METHODS OF CALCULATION

The semiempirical CNDO/S-SCF-MO model was used to calculate ground state electronic wave functions for each of the structures examined in this study. Excited states were constructed in the virtual orbital-configuration interaction (CI) approximation with 35 singly-excited configurations included in each CI calculation. Electric dipole transition integrals were calculated in the dipole velocity formalism, and all one-, two- and three-center terms were included in calculating both the electric dipole and the magnetic dipole transition moments. Rotatory strengths, dipole strengths, oscillator strengths, and dissymmetry factors were calculated for singlet-singlet transitions only.

Rotatory strengths are expressed in terms of "reduced rotatory strengths" where, for the electronic transition  $i \rightarrow j$ ,  $[R_{ij}]$  = reduced rotatory strength

$$= (100/\beta\mathcal{D}) \text{Im} \langle \psi_i | \hat{\mu} | \psi_j \rangle \cdot \langle \psi_i | \hat{m} | \psi_j \rangle. \quad (1)$$

In Eqn (1),  $\beta$  is the Bohr magneton,  $\mathcal{D}$  is the Debye unit  $\hat{\mu}$  is the electric dipole operator, and  $\hat{m}$  is the magnetic dipole operator. Dipole strengths,

$$D_i = |\langle \psi_i | \hat{\mu} | \psi_i \rangle|^2 \quad (2)$$

are expressed in Debye<sup>2</sup> ( $\mathcal{D}^2$ ) units, and dissymmetry factors are defined by:

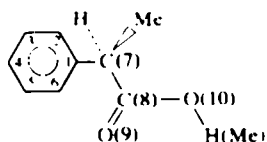
$$g_i = 4R_i/D_i \quad (3)$$

where,

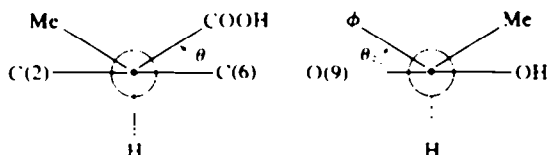
$$R_i = (\beta\mathcal{D}/100) [R_{ij}]. \quad (4)$$

#### STRUCTURES

##### (a) Hydratropic acid (1) and its methyl ester (2)

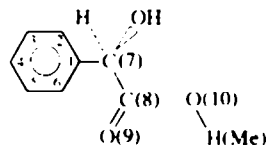


Conformational isomers of **1** and **2** were generated by varying two torsion angles,  $\theta_1$  and  $\theta_2$ , involving rotations about the C(1)-C(7) and C(7)-C(8) bonds, respectively. All other geometrical parameters (bond angles and distances) were held constant as  $\theta_1$  and  $\theta_2$  were varied. The CO bond and the O-H(Me) bond were maintained in a *cis* arrangement for all isomers. The angles  $\theta_1$  and  $\theta_2$  are defined in the following projection drawings:



When  $\theta_1 = 0^\circ$  the C(1)-C(6) and C(7)-C(8) bonds are *cis*, and when  $\theta_2 = 0^\circ$  the C(8)-O(9) and C(1)-C(7) bonds are *cis*. The angle  $\theta_1$  was varied from  $0^\circ$  to  $360^\circ$  in  $15^\circ$  increments, and  $\theta_2$  was varied over  $360^\circ$  in  $90^\circ$  increments.

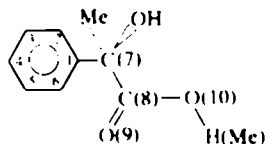
##### (b) Mandelic acid (3) and its methyl ester (4).



Conformational isomers of **3** and **4** were generated by varying the same two torsion angles as were defined above for compounds **1** and **2**. Again, all other geometrical parameters were held constant as  $\theta_1$  and  $\theta_2$  were varied. The CO bond and the O-H(Me) bond were maintained in a *cis* arrangement for all isomers, and the O-H bond of the *o*-OH substituent was directed to eclipse the C(7)-C(8) bond.

The angle  $\theta_1$  was varied from  $0^\circ$  to  $360^\circ$  in  $15^\circ$  increments, and  $\theta_2$  was varied over  $360^\circ$  in  $90^\circ$  increments.

##### (c) Atrolactic acid (5) and its methyl ester (6)



Conformational isomers of compounds **5** and **6** were generated in the same way as was described above for compounds **3** and **4**. However, due to the relatively larger sizes of **5** and **6**, calculations were carried out on fewer conformational isomers of these compounds.

#### RESULTS AND DISCUSSION

##### (a) Conformational preferences

The CNDO/S molecular orbital model was not designed (or parameterized) to provide necessarily reliable or accurate results regarding molecular conformational energies. Furthermore, since only two conformational or structural variables ( $\theta_1$  and  $\theta_2$ ) were included in the calculations reported here, our results cannot be used to draw definitive conclusions or to make definitive statements regarding conformational preferences. It is likely that the chiroptical properties of interest will be most sensitive to the variables  $\theta_1$  and  $\theta_2$ , but it is *not* certain

that these will be the most important variables in determining energy minimization. However, it is reasonable to assume that our CNDO/S-MO results may be useful in identifying the *least* favored and the *most* favored conformations (defined with respect to  $\theta_1$  and  $\theta_2$ ) and that *qualitative* use of relative conformational energies is valid.

For all the compounds studied we found that conformations with  $\theta_2 = 0^\circ$  (the CO bond pointing back towards the aromatic ring) were energetically unfavorable when  $15^\circ > \theta_1 > -15^\circ$  and  $195^\circ > \theta_1 > 165^\circ$ . This presumably may be interpreted in terms of strong repulsions between the carbonyl pi and lone-pair electrons and the pi electrons of the phenyl moiety. Near  $\theta_1 = 0^\circ$  and  $180^\circ$ , the  $\theta_2 = 0^\circ$  conformations were found to be stabilized through weak homoconjugation between the pi systems of the phenyl and carboxyl moieties. The  $\theta_2 = 180^\circ$  isomers (in which the carbonyl bond points away from the aromatic ring) were found to be more stable than the analogous  $\theta_2 = \theta^\circ$  isomers (for given values of  $\theta_1$ ), and variations in energy with  $\theta_1$  were found to be less dramatic.

For compounds 1 and 2, conformational energies for the  $\theta_2 = +90^\circ$  and  $\theta_2 = -90^\circ$  isomers were nearly identical (for a given value of  $\theta_1$ ). However, for compounds 3-4 the  $\theta_2 = -90^\circ$  isomers were much preferred (lower in energy) over the  $\theta_2 = +90^\circ$  isomers for a given value of  $\theta_1$ . This latter result can be explained in terms of a favorable intramolecular H-bonding arrangement between the  $\alpha$ -OH group and the CO oxygen atom in the  $\theta_2 = -90^\circ$  isomers. This type of arrangement would be of lesser importance in compounds 1 and 2 which do not possess a  $\alpha$ -OH group.

For 1 and 2, the most stable conformational isomers are calculated to be the following: (1)  $(\theta_1, \theta_2) = (0^\circ, 0^\circ)$ ,  $(0^\circ, 180^\circ)$ ,  $(180^\circ, 0^\circ)$  and  $(180^\circ, 180^\circ)$ ; and, (2)  $(\theta_1, \theta_2) = (\text{variable}, \pm 90^\circ)$ . For 3-6, the most stable conformational isomers are calculated to be the following: (1)  $(\theta_1, \theta_2) = (0^\circ, 0^\circ)$ ,  $(0^\circ, 180^\circ)$ ,  $(180^\circ, 0^\circ)$ , and  $(180^\circ, 180^\circ)$ ; and, (2)  $(\theta_1, \theta_2) = (\text{variable}, -90^\circ)$ . These lists of "preferred" conformational isomers are rather large and are not of great use in detailing the expected conformational mixes of the various compounds under equilibrium conditions. They merely exclude the least favorable isomers. Energy differences calculated between the so-called "preferred" isomers listed above are of the order of 0.001-0.100 eV. These differences are probably too small to be meaningful given the nature of our calculational model. Only the chiroptical properties calculated for the "preferred" conformational isomers will be discussed in subsequent sections.

### (b) $L_a$ Transition

For all the structures examined in the present study the lowest-energy singlet-singlet  $\pi \rightarrow \pi^*$  transition of the phenyl chromophore is calculated to be in the 255-265 nm region of the spectrum. Using Platt's notation,<sup>12</sup> we shall refer to this transition as  ${}^1L_a$ . In agreement with experiment, this transition is calculated to have weak oscillator strengths and weak rotatory strengths. However, whereas the oscillator strength of this transition is relatively insensitive to variations in the structural variables  $\theta_1$  and  $\theta_2$ , both the sign and the magnitude of the calculated rotatory strength are quite sensitive to changes in  $\theta_1$  and  $\theta_2$ .

The reduced rotatory strengths of the  ${}^1L_a$  transition are plotted in Fig. 1 for the  $(\theta_1, \theta_2) = (\text{variable}, \pm 90^\circ)$  conformational isomers of 1 and the  $(\theta_1, \theta_2) = (\text{variable},$

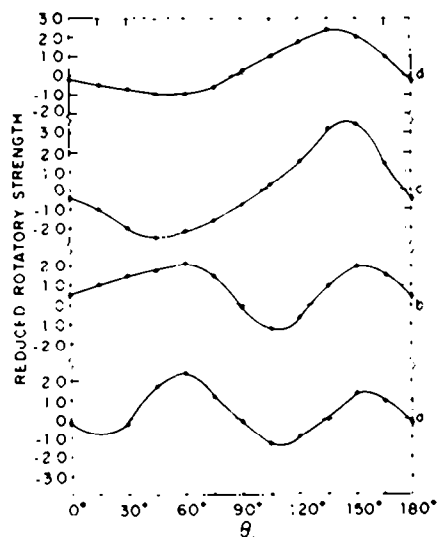


Fig. 1. Reduced rotatory strengths plotted as a function of the torsion angle  $\theta_1$  for the  ${}^1L_a$  transition in: (a) 1 ( $\theta_2 = +90^\circ$ ); (b) 1 ( $\theta_2 = -90^\circ$ ); (c) 3 ( $\theta_2 = -90^\circ$ ); and, (d) 5 ( $\theta_2 = -90^\circ$ ).

$-90^\circ$ ) conformational isomers of 3 and 5. The  ${}^1L_a$  rotatory strengths calculated for the methyl ester derivatives of 1, 3, and 5, exhibit conformational dependencies which are qualitatively similar to those found for the parent acid systems. Reduced rotatory strengths calculated for the  ${}^1L_a$  transition are listed in Table 1 for additional conformational isomers of 1, 3, 5. Again the  ${}^1L_a$  rotatory strengths calculated for the methyl ester derivatives of these compounds are qualitatively similar to those calculated for the parent acid compounds.

Experimentally, the  ${}^1L_a$  transition in 1 and 2 exhibits a positive Cotton effect for the  $S$  enantiomers.<sup>13</sup> However, the experimentally determined Cotton effect associated with the  ${}^1L_a$  transition in 3-6 is negative for the  $S$  enantiomers.<sup>14</sup> All of our calculations were carried out on the  $R$  enantiomeric forms of 1-6. The data displayed in Fig. 1 for 3 and 5 are in agreement with experiment if we assume that the conformational isomers  $(\theta_1, \theta_2) = (105^\circ - 170^\circ, \pm 90^\circ)$  predominate in solution. The  ${}^1L_a$  rotatory strengths calculated for the isomers listed in Table 1 are also compatible with experimental observation for 3 and 5. Korver *et al.* have reported that the  $(\theta_1, \theta_2) = (-135^\circ, \pm 90^\circ)$  conformational isomer is found in the solid state for  $R$ -mandelic acid (3).

Table 1. Reduced rotatory strengths calculated for the  ${}^1L_a$  transition in selected low-energy conformational isomers of compounds 1, 3 and 5

Compound	$\theta_1$	$\theta_2$	[R]
1	0	0	0.36
	0	180	0.11
	180	0	0.36
	180	180	-0.11
3	0	0	0.06
	0	180	0.31
	180	0	0.06
	180	180	0.31
5	0	0	0.12
	0	180	0.38
	180	0	0.12
	180	180	0.38

Agreement between experimental results and the theoretically calculated results for **1** and **2** is achieved only for the following conformational isomers considered in Fig. 1 and in Table 1:  $(\theta_1, \theta_2) = (0-30^\circ, 90^\circ)$ ,  $(90-135^\circ, 90^\circ)$ ,  $(90-125^\circ, -90^\circ)$ , and  $(0^\circ, 180^\circ)$ .

Korver *et al.*<sup>1</sup> have used an extended Hückel molecular orbital model to calculate the  $^1L_a$  rotatory strength of *R*-mandelic acid (**3**) as a function of the torsion angle  $\theta_1$ . Their results appear to differ significantly from those obtained by us (as plotted in Fig. 1), although a direct comparison is not possible since they did not state what value of  $\theta_2$  they assumed.

### (c) $L_a$ Transition

The phenyl localized  $^1L_a$  transition is calculated to lie in the 205–215 nm region for each of the structures examined in this study. The oscillator strengths calculated for this transition are about an order of magnitude greater than those calculated for the  $^1L_b$  transition, but are still relatively small. The rotatory strengths calculated for the  $^1L_b$  and  $^1L_a$  transitions are of the same order of magnitude.

The reduced rotatory strengths of the  $^1L_a$  transition are plotted in Fig. 2 for the  $(\theta_1, \theta_2) = (\text{variable}, \pm 90^\circ)$  conformational isomers of **1** and the  $(\theta_1, \theta_2) = (\text{variable}, -90^\circ)$  conformational isomers of **3** and **5**. The  $^1L_a$  rotatory strengths calculated for the methyl esters of **1**, **3**, and **5** exhibit conformational dependencies which are qualitatively similar to those found for the parent acid compounds. Additional reduced rotatory strengths calculated for the  $^1L_a$  transition in various low-energy conformational isomers of **1**, **3**, and **5** are listed in Table 2.

Except for conformers in which  $\theta_1$  and  $\theta_2$  are near  $0^\circ$  (or  $180^\circ$ ) (Table 2), the reduced rotatory strengths calculated for the  $^1L_a$  transition are somewhat smaller than those calculated for the  $^1L_b$  transition. This is especially true for  $\theta_1$  values where the  $^1L_b$  rotatory strengths are relatively large (and when  $\theta_2 = \pm 90^\circ$ ). The Cotton effects of the  $^1L_a$  transition in **1-6** have not been experimentally identified and characterized, so comparisons between theory and experiment are not possible in this case.

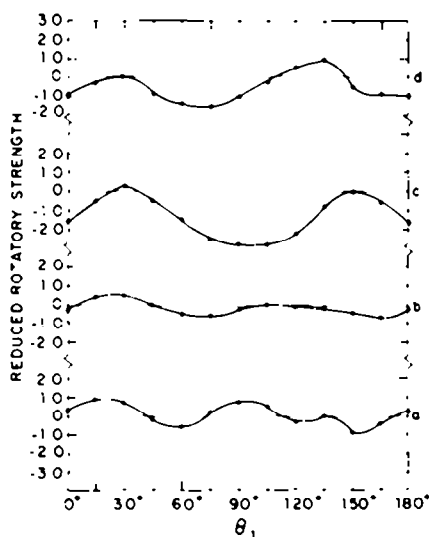


Fig. 2. Reduced rotatory strengths plotted as a function of the torsion angle  $\theta_1$  for the  $^1L_a$  transition in: (a) **1** ( $\theta_2 = -90^\circ$ ); (b) **1** ( $\theta_2 = 90^\circ$ ); (c) **3** ( $\theta_2 = -90^\circ$ ); and, (d) **5** ( $\theta_2 = -90^\circ$ ).

Table 2. Reduced rotatory strengths calculated for the  $^1L_a$  transition in selected low-energy conformational isomers of compounds **1**, **3** and **5**

Compound	$\theta_1$	$\theta_2$	[R]
<b>1</b>	0	0	-0.31
	0	180	-1.37
	180	0	-0.31
	180	180	-1.37
<b>3</b>	0	0	-1.97
	0	180	-1.08
	180	0	-1.97
	180	180	-1.80
<b>5</b>	0	0	-0.86
	0	180	-0.37
	180	0	-0.86
	180	180	0.37

### (d) Carboxyl $n \rightarrow \pi^*$ transition

In our calculations on each of the structures examined in the present study an easily identifiable transition appears which may be assigned as an  $n \rightarrow \pi^*$  excitation localized on the carboxyl moiety. In each case this transition has a relatively weak oscillator strength but a quite large rotatory strength. This transition involves excitation of an electron out of an "n" orbital on the carbonyl oxygen atom and into the carbonyl  $\pi^*$  orbital. The magnetic dipole transition integrals calculated for this transition are large (0.6–0.8 Bohr magneton) and the electric dipole transition integrals are calculated to be small. The transition energies calculated for this transition are quite sensitive to the number of singly-excited configurations included in our CI calculations. For CI basis sets <15, the transition energies fall in the 220–240 nm region. However, when the CI basis set size is increased from ~15 to 35 the transition wavelengths are pushed down into the 260–275 nm region (generally just below the calculated  $^1L_b$  transition wavelengths). The qualitative and semi-quantitative aspects of the calculated oscillator strengths and rotatory strengths are unaffected by an increase in CI basis size beyond 15. Previous calculations carried out in this laboratory on various carboxylic acid derivatives suggest that the CNDO/S-MO-CI model tends to predict  $n \rightarrow \pi^*$  transition energies which are too low by 10–30%. Previous interpretations<sup>1</sup> of the CD spectra exhibited by **1-6** have assigned the very strong Cotton effects observed in the 220–230 nm region to the carboxyl  $n \rightarrow \pi^*$  transition. We agree with this assignment and attribute the lower transition energies calculated here for the  $n \rightarrow \pi^*$  transition (for CI basis set sizes >15) to a failure in the CNDO/S-MO-CI model to accurately calculate the  $n \rightarrow \pi^*$  transition energies.

The reduced rotatory strengths calculated for the carboxyl  $n \rightarrow \pi^*$  transition are plotted in Fig. 3 for the  $(\theta_1, \theta_2) = (\text{variable}, \pm 90^\circ)$  conformational isomers of **1** and the  $(\theta_1, \theta_2) = (\text{variable}, -90^\circ)$  conformational isomers of **3** and **5**. Additional  $n \rightarrow \pi^*$  rotatory strengths are listed in Table 3 for selected low-energy conformational isomers of **1**, **3**, and **5**. Again, the methyl ester derivatives of **1**, **3**, and **5** were found to exhibit  $n \rightarrow \pi^*$  chiroptical properties similar to those calculated for the parent acids.

Experimentally the Cotton effect observed in the 220–230 nm region for **1-6** is found to be positive for the  $\delta$  enantiomers. All six compounds exhibit identically signed Cotton effects. These (presumably)  $n \rightarrow \pi^*$  Cotton effects

exhibit ellipticities which are generally about two orders of magnitude stronger than those observed for the  ${}^1L_a$  transition. Our calculated  $n \rightarrow \pi^*$  rotatory strengths are about an order of magnitude greater than the  ${}^1L_a$  rotatory strengths for corresponding conformational isomers, and a negative  $n \rightarrow \pi^*$  Cotton effect is predicted for most of the conformational isomers of the **R** enantiomeric form in 1–6 (Fig. 3 and Table 3).

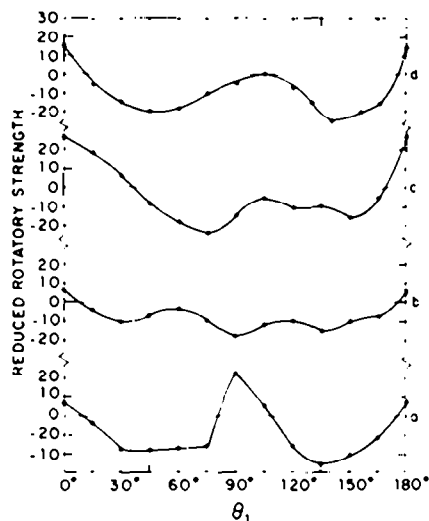


Fig. 3. Reduced rotatory strengths plotted as a function of the torsion angle  $\theta_1$  for the  $n \rightarrow \pi^*$  transition in: (a) **1** ( $\theta_2 = \pm 90^\circ$ ); (b) **1** ( $\theta_2 = -90^\circ$ ); (c) **3** ( $\theta_2 = \pm 90^\circ$ ); and, (d) **5** ( $\theta_2 = 90^\circ$ ).

Table 3. Reduced rotatory strengths calculated for the  $n \rightarrow \pi^*$  transition in selected low-energy conformational isomers of compounds 1, 3 and 5

Compound	$\theta_1$	$\theta_2$	[R]
1	0	0	1.14
	0	180	-5.69
	180	0	1.14
3	180	180	-5.69
	0	0	0.98
	0	180	-3.65
5	180	0	0.98
	180	180	3.65
	0	0	1.32
	0	180	-2.85
	180	0	1.32
	180	180	2.85

#### (e) Other transitions

In most of the structural isomers of the six compounds examined in this study the  $n \rightarrow \pi^*$  carboxyl transition and the  ${}^1L_a$  and  ${}^1L_b$  phenyl transitions lie lowest in energy. However, in certain conformational isomers in which the CO bond is pointed back towards the phenyl ring ( $\theta_2 = 0^\circ$ ) one or more low-energy ( $\lambda > 220$ ) charge-transfer transitions appear. These transitions generally involve both  $n(\text{CO}) \rightarrow \pi^*(\text{Ph})$  and  $\pi(\text{CO}) \rightarrow \pi^*(\text{Ph})$  excitations, and in some cases  $\pi(\text{Ph}) \rightarrow \pi^*(\text{CO})$  excitations are included. The excited states in these transitions are generally comprised of complicated mixtures of various configurational states in our CNDO/S-MO-CI model and are difficult to characterize precisely in simple terms. The rotatory

strengths calculated for these strongly coupled phenyl/carboxyl transitions are much weaker than those calculated for the  $n \rightarrow \pi^*$  carboxyl transition, but are of the same order of magnitude as those calculated for the  ${}^1L_a$  phenyl transition. Their oscillator strengths are calculated to be only slightly stronger than those of the  $n \rightarrow \pi^*$ ,  ${}^1L_b$ , and  ${}^1L_c$  transitions. There appears to be little evidence for the presence of these transitions in the CD and absorption spectra of 1–6 in solution media, although **5** and **6** do show a CD band in the 240 nm region (between the presumably  ${}^1L_a$  and  $n \rightarrow \pi^*$  bands) which may possibly be due to an interchromophoric (phenyl/carboxyl) charge-transfer transition. It is more likely, however, that the 240 nm CD band observed in **5** and **6** arises from a highly perturbed  $n \rightarrow \pi^*$  carboxyl transition (in one of the conformational isomers present in solution), and the strongly temperature-dependent intensity of this band would seem to support this latter interpretation.

The low-energy charge-transfer transitions do not appear in the calculations with  $\theta_2 = \pm 90^\circ$  or  $\theta_2 = 180^\circ$  (CO group pointing away from the phenyl group). In these conformations strong homoconjugation between the phenyl and carboxyl moieties is not possible.

Our study included calculations on higher energy transitions in 1–6, but these will not be discussed here. The excited states involved in these transitions were found to be complicated mixtures of phenyl  $\pi\pi^*$ , carbonyl  $\pi\pi^*$ , and phenyl/carboxyl interchromophoric charge transfer configurational states. Detailed consideration of our calculated results for these higher energy transitions is not justified given the approximations of the theoretical model employed. Most serious in this latter regard are: (a) consideration of "valence-shell-only" orbitals in the CNDO/S-MO basis set; (b) inclusion only of singly-excited configurations in the CI calculations; (c) inadequate treatment of  $\sigma - \pi$  interactions; and, (d) neglect of vibronic interactions.

#### CONCLUSIONS

The results obtained in this study suggest that the chiroptical spectra for 1–6 at  $\lambda > 205$  nm may be interpreted in terms of Cotton effects associated with the  ${}^1L_a$  and  ${}^1L_b$  phenyl localized transitions and a carboxyl localized  $n \rightarrow \pi^*$  transition. The  $n \rightarrow \pi^*$  Cotton effect is predicted to be much more intense than the  ${}^1L_a$  and  ${}^1L_b$  Cotton effects, in apparent agreement with experiment. The most consistent agreement with experimental data is achieved when it is assumed that the preferred value of  $\theta_2$  is  $90^\circ$  for the  $\alpha$ -OH substituted structures (**3–6**) and  $\pm 90^\circ$  for structures **1** and **2**. For **3–6**, a  $\theta_1$  torsion angle of  $110$ – $170^\circ$  yields results most consistent with experimental observation. For **1** and **2**, a  $\theta_1$  torsion angle near  $120^\circ$  yields results in closest agreement with experiment.

*Acknowledgements*—This work was supported by grants from the National Science Foundation, the University of Virginia Computer Science Center, and the Camille and Henry Dreyfus Foundation (through a Teacher-Scholar Award to Frederick Richardson).

#### REFERENCES

- G. Snatzke, M. Kajtar and F. Snatzke, *Fundamental Aspects and Recent Developments in Optical Rotatory Dispersion and Circular Dichroism*, (Edited by F. Ciardelli and P. Salvadori) Chap 3.4 and refs therein. Heyden (1973).
- H. Dickerson and F. S. Richardson, *J. Phys. Chem.* **80**, 2686 (1976).
- G. Barth, W. Voelter, H. S. Mosher, E. Bunnenberg and C.

- Djerassi, *J. Am. Chem. Soc.* **92**, 875 (1970).
- <sup>4</sup>O. Korver, *Tetrahedron* **26**, 5507 (1970).
- <sup>5</sup>O. Korver, S. DeJong and T. C. Van Soest, *Ibid.* **32**, 1225 (1976).
- <sup>6</sup>J. Del Bene and H. H. Jaffe, *J. Chem. Phys.* **48**, 1807 (1968); \*R. L. Ellis, G. Kuehnlenz and H. H. Jaffe, *Theoret. Chim. Acta* **26**, 131 (1972).
- <sup>7</sup>See, for example: \*F. S. Richardson, D. Shillady and J. Bloor, *J. Phys. Chem.* **75**, 2466 (1971); \*J. Linderberg and J. Michl, *J. Am. Chem. Soc.* **92**, 2619 (1970); \*J. Webb, R. Strickland and F. S. Richardson, *Ibid.* **95**, 4775 (1973).
- <sup>8</sup>See, for example: \*F. S. Richardson and D. Caliga, *Theoret. Chim. Acta* **36**, 49 (1974); \*F. S. Richardson and W. Pitts, *Biopolymers* **13**, 703 (1974); \*J. Webb, R. Strickland and F. S. Richardson, *Tetrahedron* **29**, 2499 (1973); \*F. S. Richardson and N. Cox, *J. Chem. Soc. Perkin II*, 1240 (1975); \*F. S. Richardson and W. Pitts, *Ibid. Perkin II*, 1276 (1975); \*F. S. Richardson and R. W. Strickland, *Tetrahedron* **31**, 2309 (1975).
- <sup>9</sup>See, for example: Chin-yah Yeh and F. S. Richardson, *Theoret. Chim. Acta* **39**, 197 (1975).
- <sup>10</sup>I. Tinoco, *Adv. Chem. Phys.* **4**, 113 (1962).
- <sup>11</sup>E. G. Höhn and O. E. Weigang, Jr., *J. Chem. Phys.* **48**, 1127 (1968).
- <sup>12</sup>J. Platt, *Ibid.* **17**, 484 (1949); **19**, 263 (1951).
- <sup>13</sup>F. S. Richardson and S. Ferber, *Biopolymers* **16**, 387 (1977).